

## Original Research

## Chronic myocardial infarction detection and characterization during coronary artery calcium scoring acquisitions

Gastón A. Rodríguez-Granillo, MD, PhD<sup>a,b,\*</sup>, Miguel A. Rosales, MD<sup>a</sup>,  
Renes Paola, MD<sup>■</sup>, Eduardo Diez, MD<sup>c</sup>, Jorge Pereyra, MD<sup>c</sup>, Estela Gomez, MD<sup>c</sup>,  
Gustavo De Lillo, MD<sup>c</sup>, Elina Degrossi, MD<sup>a</sup>, Alfredo E. Rodriguez, MD, PhD, FACC<sup>a</sup>,  
Eugene P. McFadden, MD, FRCPI, FACC<sup>d</sup>

<sup>a</sup>Department of Cardiovascular Imaging, Otamendi Hospital, Azcuena 870 (C1115AAB), Buenos Aires, Argentina;

<sup>b</sup>Consejo Nacional de Investigaciones Científicas y Tecnológicas (CONICET), Buenos Aires, Argentina; <sup>c</sup>Department of Radiology, Otamendi Hospital, Buenos Aires, Argentina and <sup>d</sup>Department of Interventional Cardiology, Cork University Hospital, Ireland

**KEYWORDS:**

Computed tomography;  
Infarct extension;  
Necrosis;  
Perfusion defect

**BACKGROUND:** Hypoenhanced regions on multidetector CT (MDCT) coronary angiography correlate with myocardial hyperperfusion. In addition to a limited capillary density, chronic myocardial infarction (MI) commonly contains a considerable amount of adipose tissue.

**OBJECTIVE:** We explored whether regional myocardial hypoenhancement on contrast-enhanced MDCT could be identified with standard coronary artery calcium (CAC) scoring acquisitions with non-contrast CT.

**METHODS:** Consecutive patients with a history of MI who were referred for contrast-enhanced MDCT from November 2006 until March 2009 were studied. Noncontrast CT for CAC scoring was also performed. The correlation between regional myocardial hypoenhancement on contrast-enhanced CT and regional myocardial hypoattenuated areas on noncontrast CT was defined.

**RESULTS:** Eighty-three patients (mean age, 61.5 ± 12.5 years; n = 67; 81% male) with previous MI were studied. A total of 1411 myocardial segments were evaluated. Two hundred thirty-nine segments (17%) showed myocardial hypoenhancement by MDCT and 140 segments (9.6%) by CAC. On a patient level, noncontrast CT showed a sensitivity, specificity, positive predictive value, (PPV) and negative predictive value (NPV) of 66% (95% CI, 0.53–0.77), 100% (95% CI, 0.76–1.00), 100% (95% CI, 0.90–1.00), and 41% (95% CI, 0.26–0.58), respectively, to detect myocardial hypoenhancement. On a per segment level, noncontrast CT showed a sensitivity, specificity, PPV, and NPV of 58% (95% CI, 0.51–0.64), 100% (95% CI, 0.99–1.00), 99% (95% CI, 0.94–1.00), and 92% (95% CI, 0.90–0.93), respectively, to detect myocardial hypoenhancement.

**CONCLUSIONS:** Our findings suggest that chronic MI can be detected with standard CAC scoring acquisitions.

© 2010 Society of Cardiovascular Computed Tomography. All rights reserved.

**Conflict of interest:** The authors report no conflicts of interest.  
Dr Rodríguez-Granillo received a research grant from Philips Healthcare.

\* Corresponding author.

E-mail address: [grodriuezgranillo@gmail.com](mailto:grodriuezgranillo@gmail.com)

Submitted July 20, 2009. Accepted for publication December 9, 2009.

## Introduction

The rapidly evolving field of multidetector row computed tomography coronary angiography (MDCT-CA) has led investigators to explore noncoronary applications of the technique.<sup>1</sup> In this regard, an emerging application of MDCT is the evaluation of myocardial perfusion based on the myocardial kinetics of iodinated contrast media. Parallel to gadolinium–diethylenetriamine pentaacetic acid in contrast-enhanced magnetic resonance (MR), chronic myocardial infarction (MI) and scar formation lead to impaired delivery of iodinated contrast to the infarct core because of a diminished capillary density and result in early hypoenhancement during contrast inflow.<sup>2</sup> This approach to detect MI has shown a good agreement with gated single-photon emission CT (SPECT) and contrast-enhanced MR and is highly reproducible.<sup>3–7</sup> Delayed enhancement of iodinated contrast by MDCT has been widely validated and is closely related to hypoenhanced regions with the use of contrast-enhanced MDCT.<sup>7,8</sup> In addition, both enhancement patterns are related to left ventricular function recovery.<sup>9,10</sup>

Coronary artery calcification (CAC) scoring with the use of noncontrast CT has shown a significant prognostic value to predict future coronary events independently of established risk stratification scores.<sup>11</sup> A standard CAC scoring acquisition provides an accurate estimate of the presence and severity of calcification throughout the coronary tree, requires no contrast administration, and requires a minimum radiation dose (~2 mSv). Regions of chronic MI are characterized by limited capillary density, but may also contain a considerable amount of adipose tissue and therefore may be detectable through an evaluation of myocardial attenuation on noncontrast CT.<sup>12</sup> We explore whether, in a population of patients with previous MI, myocardial hypo-enhanced regions on contrast-enhanced MDCT could also be identified by noncontrast CT performed with standard CAC scoring protocols.

## Methods

The present was a single-center, observational study of consecutive patients who were referred for MDCT evaluation at our institution from November 2006 until March 2009. Included patients had previously (>1 month) been diagnosed with MI. During the same period, patients without previous MI or revascularization who were evaluated with MDCT because of atypical chest pain or discordant stress tests were selected from our database and included as the control group. All patients included were >18 years old, in sinus rhythm, able to maintain a breathhold for  $\geq 15$  seconds, and without a history of contrast-related allergy, renal failure, or hemodynamic instability. Patients with a prescan heart rate > 70 beats/min received  $\beta$ -blockers either as a single oral dose or intravenously. Diagnosis of previous MI was made on the

basis of the history of chest pain lasting >20 minutes associated with changes on the electrocardiogram (ST-segment elevation or depression, pathologic Q waves, new onset of left bundle branch block) and abnormal levels of cardiac enzymes.

## MDCT-CA acquisition and analysis

Scans were performed with a 64-channel MDCT scanner (Brilliance 64; Philips Healthcare, Cleveland, OH). Before MDCT, all patients underwent CAC scoring with the use of a standard protocol (collimation,  $40 \times 0.625$  mm; gating at 75% R-R interval; reconstructed slice thickness, 2.5 mm; rotation time, 400 milliseconds; 120 kv, 55 mAs) corresponding to an approximate mean radiation dose of 0.67 mSv. CAC scoring is routinely performed at our institution before contrast-enhanced MDCT because, aside from its established prognostic value, it provides a reference to adjust the acquisition from the left main coronary artery up to the posterior descending artery to adjust scan length. For MDCT acquisition, a bolus of 80–120 mL of iodinated contrast material (Optiray; ioversol 350 mg/mL; Mallinckrodt, St Louis, MO) was injected through an arm vein at 5–6 mL/s. A bolus tracking technique was used to synchronize the arrival of contrast at the level of the coronary arteries with the start of acquisition. Scan parameters of the MDCT acquisitions were a collimation of  $64 \times 0.625$  mm, rotation time of 0.42 seconds, tube voltage of 120 kV, and tube current of 600–1000 mAs corresponding to an approximate mean radiation dose of 12 mSv. A dose modulation protocol was applied to reduce radiation dose during systole whenever deemed possible by the operator,<sup>13</sup> with an approximate dose saving of 42% at a heart rate of 60 beats/min, yielding an approximate mean radiation dose of 7 mSv in these patients. An electrocardiogram was recorded simultaneous to the CT scan to enable retrospective gating of the image data. A dedicated cardiac gating algorithm was used that identified the same physiologic phases of the cardiac cycle while taking into account the nonlinear changes in the individual cardiac states with the heart rate variations during the CT acquisition.<sup>14</sup>

CAC scoring acquisition was reconstructed at 75% of the R-R interval with the use of axial planes and multiplanar reconstructions. Short-axis (from base to apex) and 4-chamber views were obtained, and the presence of myocardial hypoattenuation was evaluated.

MDCT images were reconstructed at 75% of the cardiac phase with the use of axial planes, multiplanar reconstructions, and maximum intensity projections at 1-mm slice thickness. Short-axis (from base to apex) and 2-, 3-, and 4-chamber views were obtained initially with the use of 5-mm slice reformatted images. The presence of myocardial hypoenhancement was evaluated by consensus of 2 experienced observers and defined as myocardium having a signal density 2 standard deviations below the mean myocardial signal density of the remote myocardium. The

number or segments with myocardial hypoenhancement was assessed by using the American Heart Association (AHA) 17-segment model.<sup>15</sup> Attenuation levels (Hounsfield unit; HU) of the region of MI, remote myocardium, and pericardial fat were estimated after averaging measurements at 3 regions of interest. For cases with myocardial wall calcification, attenuation was measured at noncalcified regions in the vicinity.

Left ventricular ejection fraction (LVEF) was assessed by using Simpson's method of discs,<sup>16</sup> and myocardial contractility was evaluated as previously described.<sup>17</sup> All analyses were performed with the use of dedicated software (Comprehensive Cardiac Analysis, Version 3.5), on a CT workstation (Brilliance Workspace; Philips Healthcare). The study was approved by our Institution's Ethics Committee, and all the patients enrolled gave their written informed consent.

### Statistical analysis

Discrete variables are presented as counts and percentages. Continuous variables are presented as mean  $\pm$  SD or median (interquartile range), as indicated. Comparisons among groups were performed with the use of paired samples *t* test, independent samples *t* test, analysis of variance, Mann-Whitney *U* tests, chi-square tests, or Fisher's exact test as indicated. MDCT served as the reference standard for the diagnosis of regional MI. Diagnostic performance and predictive value of CAC for the diagnosis of regions showing MI compared with the reference standard was evaluated on a per patient level and per segment level and expressed as sensitivity, specificity, positive predictive value (PPV), and negative predictive value (NPV) and their corresponding 95% confidence intervals. We explored correlations between the LVEF and the number of hypoenhanced segments with the use of Pearson's and Spearman's correlation coefficients, as indicated. Agreement between observers and methods was compared with  $\kappa$  statistics. A 2-sided *P* value of less than 0.05 indicated statistical significance. Statistical analyses were performed with use of SPSS software, Version 13.0 (Chicago, IL).

### Results

One hundred forty-three patients were studied, including 83 patients with a previous MI and 60 controls. The mean age was  $59.4 \pm 12.1$  years, 113 (79%) were male, and 10 (7%) were diabetic. As expected, patients with previous MI had larger burden of cardiovascular risk factors (Table 1). Sixty-seven patients (81%) with previous MI had previously undergone percutaneous coronary intervention, and 8 (6%) had previous bypass surgery. Forty-three patients (52%) were studied for evaluation of revascularization procedures, 33 (40%) because of chest pain and 7 (8%) because of discordant stress tests. Among the control

group, 20 patients (33%) were studied because of the presence of multiple risk factors, 22 (37%) because of atypical chest pain, and 18 (30%) because of inconclusive stress tests. Demographic characteristics of patients are presented in Table 1. Patients in the control group had a median Agatston score of 0.0 (interquartile range, 0–49), with a median number of calcified lesions of 0.5 (interquartile range, 0–3).

### Myocardial hypoenhancement detection with CAC and MDCT

A total of 2431 left ventricular AHA segments were evaluated, all being judged analyzable by contrast and noncontrast CT. In the control group, 4 segments (0.4%) in 4 patients (7%) showed myocardial hypoenhancement, involving the same (inferobasal) segment in all cases. In addition, those patients had no hypoenhancement on non-contrast CT. In turn, in patients with previous MI, 239 segments (17%) within 67 patients (81%) showed hypoenhancement at MDCT. In those patients, noncontrast CT detected myocardial hypoenhancement in 140 segments (9.6%) within 44 patients (53%) (Figure 1, Figure 2, and Figure 3). Demographic characteristics were not related to the presence of myocardial hypoenhancement on MDCT (Table 2).

MDCT identified intraventricular thrombus (Figure 2) in 9 patients (11%) and was calcified in 3 (33%) of 9 patients. Myocardial wall thinning (Figure 2 and Figure 3) and calcification (Figure 3) was present in 56 (68%) and 3 (4%) patients, respectively. An apical aneurysm was found in 4 patients (5%). These morphologic findings (Table 1), despite the presence of calcification, were undetected by noncontrast CT.

On a per patient level and using MDCT as the reference standard, noncontrast CT showed a sensitivity of 66% (95% CI, 0.53–0.77), specificity of 100% (95% CI, 0.76–1.00), PPV of 100% (95% CI, 0.90–1.00), and NPV of 41% (95% CI, 0.26–0.58) to detect regions of myocardial hypoenhancement on contrast CT. On a per segment level, noncontrast CT showed a sensitivity of 58% (95% CI, 0.51–0.64), specificity of 100% (95% CI, 0.99–1.00), PPV of 99% (95% CI, 0.94–1.00), and NPV of 92% (95% CI, 0.90–0.93) to detect regions of myocardial hypoenhancement on contrast CT. There was good agreement in the identification of hypoenhanced segments between contrast and noncontrast CT, respectively, on a segmental basis ( $\kappa = 0.69$ ,  $P < 0.001$ ).

Patients with concordant contrast and noncontrast CT findings had significantly older infarcts than patients with discordant findings (24 months; interquartile range, 10–57 months versus 12 months; interquartile range, 6–24 months;  $P = 0.016$ ).

To assess interobserver agreement in the detection of myocardial hypoattenuation, 28 randomly selected cases

**Table 1** Demographical characteristics

	Total (n = 143)	Previous MI (n = 83)	Control (n = 60)	P
Age, y, mean $\pm$ SD	59.4 $\pm$ 12.1	61.5 $\pm$ 12.8	56.5 $\pm$ 10.4	0.02
Male, n (%)	113 (79)	67 (81)	46 (77)	0.68
Hypertension, n (%)	77 (54)	51 (61)	26 (43)	0.04
Hypercholesterolemia, n (%)	92 (64)	57 (69)	35 (58)	0.22
Former smoker, n (%)	42 (29)	27 (33)	15 (25)	0.11*
Current smoker, n (%)	17 (12)	6 (7)	11 (18)	
Diabetes, n (%)	10 (7)	7 (8)	3 (5)	0.52
Previous MI, n (%)	83 (58)	83 (100)	0 (0)	<0.001
Previous PCI, n (%)	67 (47)	67 (81)	0 (0)	<0.001
Previous CABG, n (%)	8 (6)	8 (10)	0 (0)	0.02
Heart rate, beats/min, mean $\pm$ SD	60.2 $\pm$ 6.9	60.6 $\pm$ 7.0	59.6 $\pm$ 6.8	0.37
Infarct age, mo, median (interquartile range)		24.0 (7.0–48.0)		
MDCT structural findings				
LVEF, mean $\pm$ SD	55.1 $\pm$ 9.6	50.9 $\pm$ 9.7	61.0 $\pm$ 5.5	<0.001
Hypoenhancement, n (%)	71 (50)	67 (81)	4 (7)	<0.001
LV thrombus, n (%)	9 (6)	9 (11)	0 (0)	0.01
Wall thinning, n (%)	59 (39)	56 (68)	0 (0)	<0.001
Wall calcification, n (%)	3 (2)	3 (4)	0 (0)	0.26
Aneurysm, n (%)	4 (3)	4 (5)	0 (0)	0.14
Wall motion abnormalities, n (%)	67 (47)	66 (80)	1 (2)	<0.001

PCI, percutaneous coronary intervention; CABG, coronary artery bypass graft; LV, left ventricular.

\*Chi-square across group.

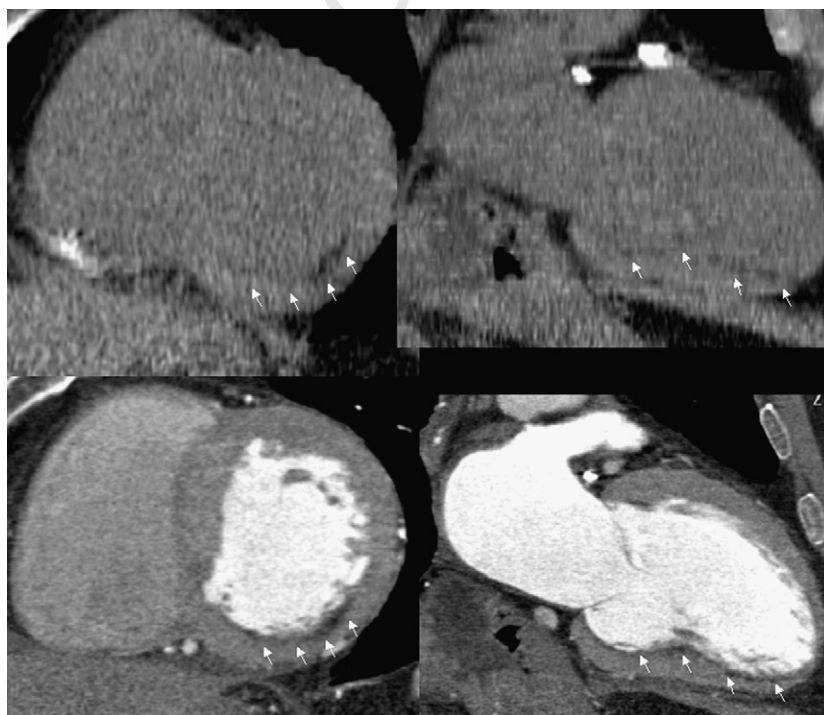


**Figure 1** Inferior subendocardial infarction assessed by short-axis views (*left*) and long vertical-axis views (*right*) with the use of CAC scoring acquisition (*top*) and MDCT-CA (*bottom*). CAC hypoattenuation correlates well with hypoenhancement at contrast-enhanced MDCT (*arrows*).



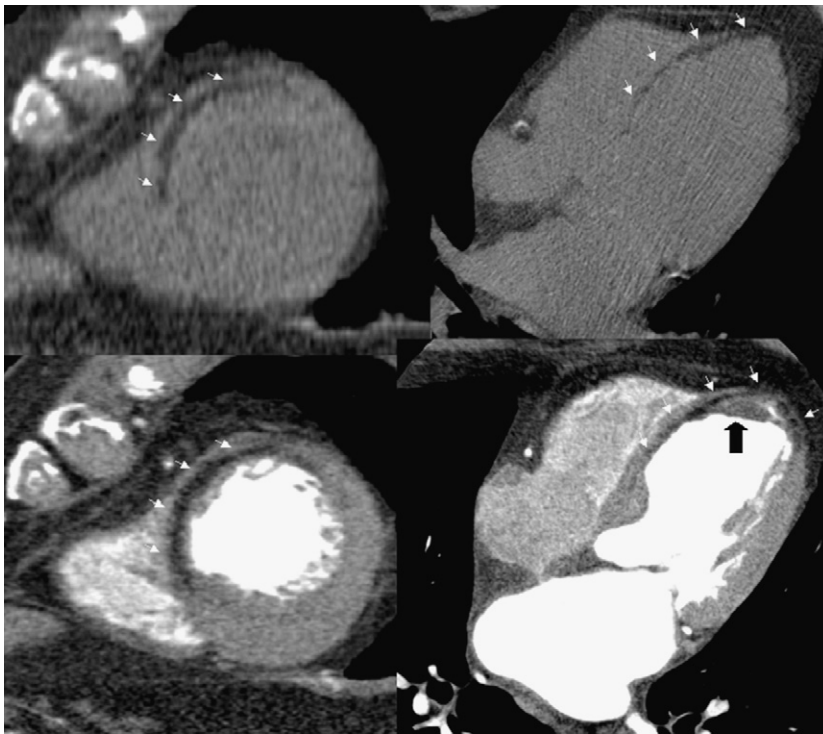


**Figure 2** Anteroseptal transmural infarction assessed by short-axis views (*left*) and horizontal long-axis views (*right*) by CAC scoring acquisition (*top*) and MDCT-CA (*bottom*). Significant myocardial wall thinning and apical thrombus (*black arrow*) are observed in MDCT (*bottom*).

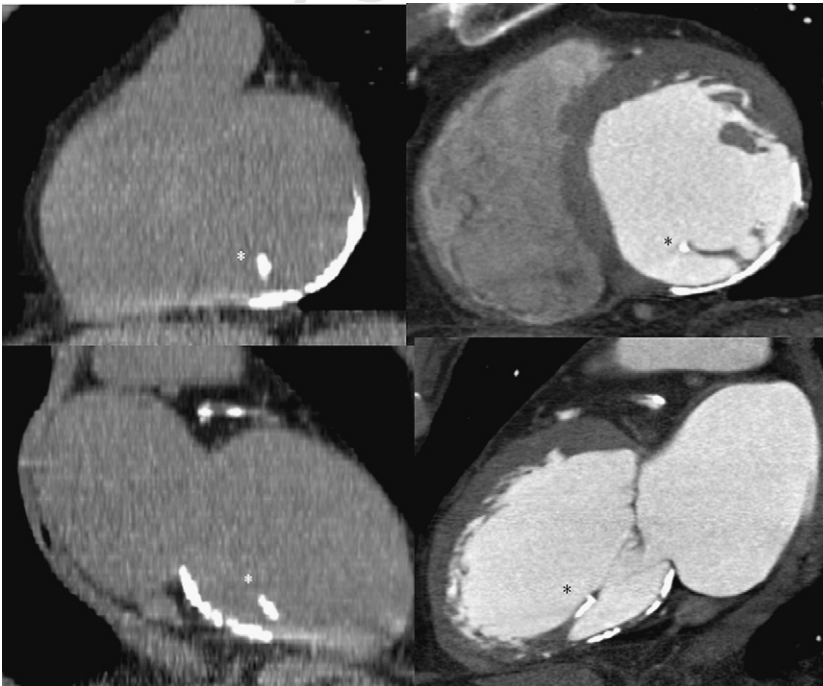


**Figure 3** Inferior transmural infarction assessed by short-axis views (*top*) and long vertical-axis views (*bottom*) by CAC scoring acquisition (*left*) and MDCT-CA (*right*). Myocardial wall thinning and calcification can be detected by both techniques. Calcification of the posteromedial papillary muscle (\*) can be appreciated.

**Table 2** Relationship between demographic and procedural characteristics and the presence of myocardial hypoenhancement by MDCT

	Present (n = 67)	Absent (n = 16)	P
Age, y, mean ± SD	62.1 ± 12.4	58.6 ± 14.3	0.33
Male, n (%)	54 (81)	13 (81)	0.95
Hypertension, n (%)	42 (63)	9 (56)	0.78
Hypercholesterolemia, n (%)	47 (70)	10 (63)	0.56
Former smoker, n (%)	21 (31)	6 (38)	0.53*
Current smoker, n (%)	4 (6)	2 (13)	
Diabetes, n (%)	6 (9)	1 (6)	0.99
Previous PCI, n (%)	53 (79)	14 (88)	0.73
Previous CABG, n (%)	7 (10)	1 (6)	0.99
Heart rate, beats/min, mean ± SD	60.4 ± 6.6	61.6 ± 8.6	0.53
LVEF, %, mean ± SD	49.9 ± 10.0	55.3 ± 7.1	0.02
Clinical presentation			0.21*
Control of revascularization, n (%)	32 (48)	11 (69)	
Chest pain, n (%)	28 (42)	5 (31)	
Inconclusive stress test, n (%)	7 (10)	0 (0)	

PCI, percutaneous coronary intervention; CABG, coronary artery bypass graft.

\*Chi-square across group.

(476 left ventricular segments) were analyzed independently by 2 experienced observers, and a good agreement was found for both noncontrast CT ( $\kappa = 0.88$ ,  $P < 0.001$ ) and contrast-enhanced MDCT ( $\kappa = 0.85$ ,  $P < 0.001$ ).

### Difference in attenuation levels between necrosis and pericardial fat

Attenuation levels in regions of MI were predominantly negative on both contrast-enhanced and noncontrast CT ( $-20.7 \pm 37.4$  HU versus  $-10.8 \pm 29.8$  HU;  $P < 0.001$ ). Nevertheless, pericardial fat showed significantly lower attenuation levels than did necrotic regions (Table 3).

Attenuation levels in regions remote to the area of MI were significantly higher than attenuation levels of necrotic segments with both contrast ( $112.6 \pm 19.4$  HU versus  $-20.7 \pm 37.4$  HU;  $P < 0.001$ ) and noncontrast CT ( $43.3 \pm 10.5$  HU versus  $-10.8 \pm 29.8$  HU;  $P < 0.001$ ) (Table 3). The difference in attenuation levels between regions of MI and remote myocardium was significantly higher

when measured by contrast than by noncontrast CT ( $133.3 \pm 41.1$  HU versus  $54.2 \pm 29.0$  HU;  $P < 0.001$ ).

### MI, infarct age, and LVEF

The mean LVEF was  $55.1\% \pm 9.6\%$  and was significantly higher in the control group ( $61.0\% \pm 5.5\%$  versus  $50.9\% \pm 9.7\%$ ;  $P < 0.001$ ). Among patients with previous MI, patients without hypoenhancement had significantly higher LVEF than patients with myocardial necrosis ( $55.3\% \pm 7.1\%$  versus  $49.9\% \pm 10.0\%$ ;  $P = 0.02$ ) (Table 1 and Table 2). Figure 4 shows the significant inverse relationship between the number of AHA segments with hypoenhancement and the LVEF identified with both noncontrast ( $r = -0.49$ ,  $P < 0.001$ ) and contrast-enhanced CT ( $r = -0.50$ ,  $P < 0.001$ ). Patients with myocardial hypoenhancement on contrast CT had older infarcts than did patients without hypoenhancement (24 months; interquartile range, 12–48 months versus 6 months; interquartile range, 3–33 months;  $P = 0.04$ ). Similarly, results were

**Table 3** Difference in myocardial attenuation levels at the necrotic region and at the remote myocardium between CAC scoring acquisition and MDCT-CA acquisition and difference in attenuation levels between pericardial fat and necrosis measured with CAC and MDCT

	CAC	MDCT	P	Fat CAC	P vs MI CAC	Fat MDCT	P vs MI CAC
Attenuation MI, HU, mean ± SD	$-10.8 \pm 29.8$	$-20.7 \pm 37.4$	$<0.001$	$-105.4 \pm 14.8$	$<0.001$	$-104.6 \pm 18.2$	$<0.001$
Attenuation remote, HU, mean ± SD	$43.3 \pm 10.5$	$112.6 \pm 19.4$	$<0.001$				
Difference MI/remote, mean ± SD	$54.2 \pm 29.0$	$133.3 \pm 41.1$	$<0.001$				
P	$<0.001$	$<0.001$					

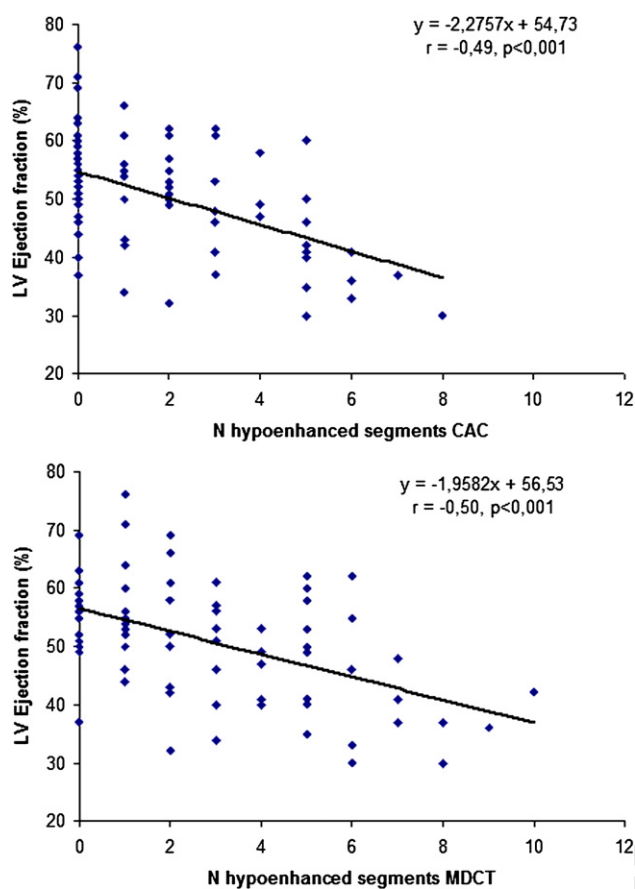


**Figure 4** Relationship between the number of hypoattenuated segments and the LVEF with the use of CAC (*top*) and multidetector MDCT-CA (*bottom*).

found with noncontrast CT. Hypoattenuated segments detected by noncontrast CT corresponded to older MIs than those detected by contrast CT (Table 4).

## Discussion

Several studies have established that hypoenhanced regions on contrast-enhanced MDCT correlate well to hypoperfused myocardial regions, becoming an accurate tool to evaluate MI, with a good agreement with gated SPECT and MR.<sup>2-7</sup> Indeed, MDCT allows assessment of morphologic characteristics and extension of both chronic

and acute MIs.<sup>4,18</sup> In the present study, we hypothesized that hypoenhanced areas at MDCT could be identified by standard, noncontrast CT CAC scoring protocols because, other than a reduced capillary density, healed MIs contain adipose tissue and should therefore be hypoattenuated on CAC.<sup>12</sup>

The main finding of the present study was that hypoenhanced areas detected with the use of MDCT-CA in patients with chronic MI can be detected as hypoattenuated areas with the use of standard CAC scoring acquisitions. Despite a moderate sensitivity, CAC showed an excellent specificity to detect myocardial hypoenhancement by MDCT. Our results are further supported by the findings in the control group that show myocardial hypoenhancement in only 0.4% of myocardial segments assessed by MDCT, all involving the inferobasal segment. Furthermore, no myocardial hypoattenuation was detected by noncontrast CT imaging in control patients. These results are in keeping with a recent report from our group showing that beam-hardening artifact from the spine can mimic myocardial perfusion defects that affect particularly those segments.<sup>19</sup>

The histopathologic evolution of MI is not fully elucidated. Su et al<sup>12</sup> found that 84% of healed MIs contain adipose tissue. In keeping with that, we found that attenuation levels at necrotic regions were predominantly negative, ranging between -10 HU and -20 HU with the use of CAC and MDCT protocols, respectively. These attenuation levels were significantly higher than attenuation levels of pericardial fat, that were around -100 HU with the use of CAC and MDCT protocols. In turn, remote myocardium showed significantly higher attenuation levels that ranged between 43 HU and 112 HU with the use of CAC and MDCT protocols, respectively. These findings reinforces the recent concept that MI is characterized mainly by adipose tissue probably interspersed between fibrotic fibers and rarely evolves to calcification.<sup>12,19-21</sup> Accordingly,<sup>3</sup> the concept of myocardial scar, that has been long deemed mainly dense fibrotic tissue, should probably be revisited.

The presence of myocardial necrosis had a correlate in left ventricular function, because patients with myocardial hypoenhancement showed significantly lower LVEF than patients without myocardial hypoenhancement. In addition, an inverse relationship was found between the extent of necrosis and the LVEF. In line with a previous study that

**Table 4** Relationship between infarct age (in months) with the presence or absence of myocardial hypoenhancement with the use of CAC and MDCT

	Myocardial hypoenhancement		P
	Present	Absent	
CAC, median (interquartile range)	36.0 (13.3-60.0)	11.0 (4.0-24.0)	<0.001
MDCT, median (interquartile range)	24.0 (12.0-48.0)	5.5 (3.0-33.0)	0.04
P	<0.001	<0.001	

related the presence of adipose tissue within healed myocardium to older age,<sup>12</sup> we found that MI segments detected by noncontrast CT corresponded to older MIs than those detected by contrast-enhanced CT. Twenty-seven percent of patients with myocardial hypoenhancement on contrast-enhanced MDCT did not show hypoattenuation on noncontrast CT, a finding that could be ascribed to the absence of adipose tissue in patients with relatively recent infarcts. In parallel, 19% of our patients with MI did not show abnormalities on contrast-enhanced MDCT possibly because of false negatives or to patients with a smaller MI.<sup>9</sup>

Overall, our findings suggest that chronic MI might be detected by standard CAC scoring acquisitions. It should be noted that once it has been established that a patient has a prior MI, the need to screen for CAC is less clear. Thus, if routine CAC screening was able to identify prior MI, the true benefit would be identifying patients with unrecognized prior MI. As expected, contrast-enhanced MDCT provided much more detail into the evaluation of the morphologic characteristics, extent, and complications of MI such as thrombus and aneurysm formation. Nevertheless, our results could potentially add prognostic value of the technique.

## Limitations

Because we performed a retrospective evaluation of patients with previous MI, selection bias may be present and caution must be taken to interpret predictive values particularly on a per patient basis because they are influenced by the prevalence of the disease. In addition, potential for nesting effects within segmental analysis should not be disregarded. Larger prospective studies with clinically driven as well as global and regional LV function parameters at follow-up would provide insight into the clinical significance of our findings. Finally, although it has been validated as an accurate tool to identify the presence and extent of MI, MDCT has been shown to slightly overestimate infarct size.<sup>2,7</sup> Therefore, studies that used <sup>99m</sup>Tc-sestamibi-gated SPECT or cardiac MR as reference standard are warranted.

## Conclusions

Our findings suggest that chronic MI can be detected with the use of standard CAC scoring acquisitions.

## References

1. Tops LF, Krishnan SC, Schuijff JD, Schalij MJ, Bax JJ: Noncoronary applications of cardiac multidetector row computed tomography. *J Am Coll Cardiol Imaging*. 2008;1:94-106.
2. Hoffmann U, Millea R, Enzweiler C, Ferencik M, Gulick S, Titus J, Achenbach S, Kwait D, Sosnovik D, Brady TJ: Acute myocardial infarction: contrast-enhanced multidetector row CT in a porcine model. *Radiology*. 2004;231:697-701.
3. Baks T, Cademartiri F, Moelker AD, Weustink AC, van Geuns RJ, Mollet NR, Krestin GP, Duncker DJ, de Feyter PJ: Multislice computed tomography and magnetic resonance imaging for the assessment of reperfused acute myocardial infarction. *J Am Coll Cardiol*. 2006;48:144-52.
4. Gerber BL, Belge B, Legros GJ, Lim P, Poncelet A, Pasquet A, Gisellu G, Coche E, Vanoverschelde JL: Characterization of acute and chronic myocardial infarcts by multidetector computed tomography: comparison with contrast-enhanced magnetic resonance. *Circulation*. 2006;113:823-33.
5. Henneman MM, Schuijff JD, Jukema JW, Lamb HJ, de Roos A, Dibbets P, Stokkel MP, van der Wall EE, Bax JJ: Comprehensive cardiac assessment with multislice computed tomography: evaluation of left ventricular function and perfusion in addition to coronary anatomy in patients with previous myocardial infarction. *Heart*. 2006;92:1779-83.
6. Nikolaou K, Sanz J, Poon M, Wintersperger BJ, Ohnesorge B, Uius T, Faya ZA, Reiser MF, Becker CR: Assessment of myocardial perfusion and viability from routine contrast enhanced 16-detector-row computed tomography of the heart: preliminary results. *Eur Radiol*. 2005;15:864-71.
7. Mahnken AH, Bruners P, Katoh M, Wildberger JE, Gunther RW, Buecker A: Dynamic multi-section CT imaging in acute myocardial infarction: preliminary animal experience. *Eur Radiol*. 2006;16:746-52.
8. Lardo AC, Cordeiro MA, Silva C, Amado LC, George RT, Saliaris AP, Schuler KH, Fernandes VR, Zviman M, Nazarian S, Halperin HR, Wu KC, Hare JM, Lima JA: Contrast-enhanced multidetector computed tomography viability imaging after myocardial infarction: characterization of myocyte death, microvascular obstruction, and chronic scar. *Circulation*. 2006;113:394-404.
9. Rodriguez-Granillo GA, Rosales MA, Baum S, Rennes P, Rodriguez-Pagani C, Curotto V, Fernandez-Pereira C, Llaurado C, Risau G, Degrossi E, Doval HC, Rodriguez AE: Early assessment of myocardial viability using delayed enhancement 64-channel CT after primary PCI: relationship with clinical and angiographical parameters of reperfusion. *J Am Coll Cardiol Imaging*. 2009;2:1072-81.
10. Lessick J, Dragu R, Mutlak D, Rispler S, Beyar R, Litmanovich D, Engel A, Agmon Y, Kapeliovich M, Hammerman H, Ghersin E: Is functional improvement after myocardial infarction predicted with myocardial enhancement patterns at multidetector CT? *Radiology*. 2007;244:736-44.
11. Detrano R, Guerci AD, Carr JJ, Bild DE, Burke GB, Folsom AR, Liu K, Shea S, Szklo M, Bluemke DA, O'Leary DH, Tracy R, Watson K, Wong ND, Kronmal RA: Coronary calcium as a predictor of coronary events in four racial or ethnic groups. *N Engl J Med*. 2008;358:1336-45.
12. Su L, Siegel JE, Fishbein MC: Adipose tissue in myocardial infarction. *Cardiovasc Pathol*. 2004;13:98-102.
13. Hausleiter J, Meyer T, Hadamitzky M, Huber E, Zankl M, Martinoff S, Kastrati A, Schomig A: Radiation dose estimates from cardiac multislice computed tomography in daily practice: impact of different scanning protocols on effective dose estimates. *Circulation*. 2006;113:1305-10.
14. Vembar M, Garcia MJ, Heuscher DJ, Haberl R, Matthews D, Bohme GE, Greenberg NL: A dynamic approach to identifying desired physiological phases for cardiac imaging using multislice spiral CT. *Med Phys*. 2003;30:1683-93.
15. Cerqueira MD, Weissman NJ, Dilsizian V, Jacobs AK, Kaul S, Laskey WK, Pennell DJ, Rumberger JA, Ryan T, Verani MS: Standardized myocardial segmentation and nomenclature for tomographic imaging of the heart: a statement for healthcare professionals from the Cardiac Imaging Committee of the Council on Clinical Cardiology of the American Heart Association. *Circulation*. 2002;105:539-42.
16. Lin FY, Devereux RB, Roman MJ, Meng J, Jow VM, Jacobs A, Weinsaft JW, Shaw LJ, Berman DS, Callister TQ, Min JK: Cardiac chamber volumes, function, and mass as determined by 64-multidetector row computed tomography: mean values among healthy adults free of hypertension and obesity. *J Am Coll Cardiol Imaging*. 2008;1:782-6.
17. Henneman MM, Bax JJ, Schuijff JD, Jukema JW, Holman ER, Stokkel MP, Lab HJ, de Roos A, van der All EE: Global and regional



left ventricular function: a comparison between gated SPECT, 2D echocardiography and multi-slice computed tomography. *Eur J Nucl Med Mol Imaging*. 2006;33:1452–60.

18. Nieman K, Cury RC, Ferencik M, Nomura CH, Abbara S, Hoffmann U, Gold HK, Jang IK, Brady TJ: Differentiation of recent and chronic myocardial infarction by cardiac computed tomography. *Am J Cardiol*. 2006;98:303–8.
19. Rodríguez-Granillo GA, Rosales MA, Degrossi E, Rodríguez AE: Signal density of left ventricular myocardial segments and impact of beam hardening artifact: implications for myocardial perfusion

assessment by multidetector CT coronary angiography [published online ahead of print November 12, 2009]. *Int J Cardiovasc Imaging*. Doi:10.1007/s10554-009-9531-5.

20. Zafar H, Litt HI, Totigian DA: CT imaging of left ventricular myocardial fat in patients with CT findings of chronic left ventricular myocardial infarction. *Clin Radiol*. 2008;63(3):256–62.
21. Raney AR, Saremi F, Kenchaiah S, Gurudevan SV, Narula J, Narula N, Channal S: Multidetector computed tomography shows intramyocardial fat deposition. *J Cardiovasc Comput Tomogr*. 2008;2:152–63.

UNCORRECTED PROOF

935  
936  
937  
938  
939  
940  
941  
942  
943  
944  
945  
946  
947  
948  
949  
950  
951  
952  
953  
954  
955  
956  
957  
958  
959  
960  
961  
962  
963  
964  
965  
966  
967  
968  
969  
970  
971  
972  
973  
974  
975  
976  
977  
978  
979  
980  
981  
982  
983  
984  
985  
986  
987  
988  
989  
990